Slow Dielectric Relaxation of a Styrene−Isoprene−Styrene Triblock Copolymer with Dipole Inversion in the Middle Block: A Challenge to a Loop/Bridge Problem

Hiroshi Watanabe[†]

Institute for Chemical Research, Kyoto University, Uji, Kyoto 611, Japan

Received March 20, 1995[⊗]

ABSTRACT: Dielectric behavior was investigated for *lamellar-forming* polystyrene−polyisoprene−polystyrene (PS−PI−PS) triblock and PS−PI diblock copolymers, the latter being identical to the half-contour of the former. The *end* PI block of PS−PI had type-A dipoles parallel in the same direction along its contour, while the *middle* PI block of PS−PI−PS had type-A dipoles *inverted* at its center. Those type-A dipoles enabled us to dielectrically observe the global motion of the PI blocks *connected to* the *glassy PS domains*. The dipole inversion was an absolute requirement for this observation for the middle PI blocks having a fixed end-to-end vector **R**: For the middle blocks without the inversion, the polarization ($\propto$**R**) does not fluctuate and the global motion is dielectrically inert. The end PI block of PS−PI took only a tail conformation, while the middle PI block of PS−PI−PS took either a loop or a bridge conformation. For evaluation of the bridge fraction for the latter, dielectric loss (ϵ'') curves were compared for the end and middle PI blocks before and after imposition of a large-amplitude (γ_0) oscillatory shear, and the shear effects on the viscoelastic properties and lamellar alignment were also examined. Before the large-γ_0 shear, the end and middle PI blocks exhibited nearly the same dielectric relaxation mode distribution *at long time scales* but the relaxation intensity was larger for the former by a factor $\lambda_v = 1.7$. An argument of similarity of behavior of the tail and loop led us to assign the slow relaxation of the middle block to the loop relaxation, giving an estimate for the bridge fraction $\phi_{bridge} \cong (\lambda_v - 1)/\lambda_v \cong 40\%$. Equilibrium theories successfully explained this ϕ_{bridge} value. For PS−PI the large-γ_0 shear significantly decreased the viscoelastic moduli, improved the lamellar alignment a little, but hardly affected the dielectric behavior. On the other hand, for PS−PI−PS the shear hardly affected the moduli and lamellar alignment but increased the dielectric relaxation intensity at long time scales. These differences between PS−PI and PS−PI−PS suggested that the shear decreased ϕ_{bridge} for the latter because it preferred the PS−PI−PS loop generating smaller stress as compared to the PS−PI−PS bridge. Thus, the observed shear effects were in harmony with the above assignment for the slow relaxation of the middle block.

Introduction

Strongly segregated block copolymers exhibit various microdomain structures. For B−A type diblock copolymers, the dependence of the microdomain shape and size on the block molecular weights and composition has been extensively studied,[1−5] and good agreements with thermodynamic theories[6−9] have been found[1,5] (except for spherical domains[10]). On the other hand, for B−A−B type *symmetrical* triblock copolymers, the microdomain structures have been considered to be identical to those of B−A/2 type diblock copolymers.[1,11] In fact, coincidence of the domain size has been confirmed for B−A−B and B−A/2 copolymers.[1,4]

Despite this similarity of the domain structures, a well-known, important difference exists for the chain conformation of B−A diblock and B−A−B triblock copolymers: The diblock copolymers have only *end* blocks that always take a *tail* conformation (part a of Figure 1), while the triblock copolymers have a *middle* block that can be either a *loop* having two ends connected to the same B domain or a *bridge* connecting different B domains (parts b and c). Thus, the structure of the triblock copolymers has to be specified for both microdomains and chain conformation, the latter being characterized with the bridge fraction ϕ_{bridge}. This fraction should significantly influence viscoelasticity,[12] mechanical strength, and other physical properties of triblock copolymers that are often used as thermoplastic elastomers. Theoretical efforts have been made to evaluate ϕ_{bridge}.[13−17] However, as far as the author knows, no reliable ϕ_{bridge} data have been reported, mostly because of a lack of simple experimental methods for determining ϕ_{bridge}.

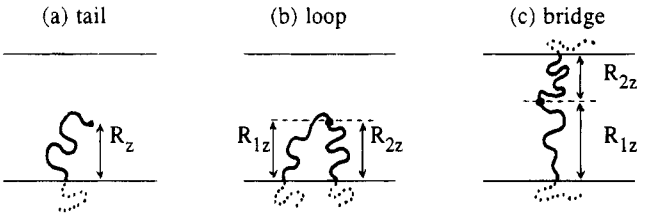

Figure 1. Schematic illustration of (a) tail-PI for PS−PI, (b) loop-PI for PS−PI−PS, and (c) bridge-PI for PS−PI−PS.

As one possible approach to this problem, a dielectric method may be useful if the middle block has *type-A* dipoles[18,19] aligned parallel to the chain contour. As pioneered by Stockmayer et al.[18,19] and later examined extensively by several groups,[20−25] type-A dipoles enable us to dielectrically observe the global chain motion. At this point, we note that this observation is not so trivial for the middle blocks having fixed ends (as is the case studied here): Usual type-A chains have dipoles aligned in the same direction along their contour so that the polarization **P** is proportional to the end-to-end vector **R**. If the ends are fixed for those chains, **R** does not fluctuate and thus the global motion is dielectrically inert. This difficulty is removed if we introduce an *inversion* of the type-A dipoles. The resulting chains have **P** being proportional to a difference between two end-to-center vectors and their global motion induces the dielectric relaxation even when **R** does not fluctuate. This relaxation behavior should be different for the loop-

[†] Previously at Osaka University.
[⊗] Abstract published in *Advance ACS Abstracts,* June 1, 1995.

0024-9297/95/2228-5006$09.00/0

Table 1. Characteristics of the PS–PI and PS–PI–PS Samples

code	$10^{-3}M_{PS}$	$10^{-3}M_{PI}$	M_w/M_n
PS–PI 12–12	11.7	11.6	1.04
PS–PI–PS 12–$(12)_2$–12[a]	23.4[b]	23.2	1.05

[a] Symmetric triblock copolymer having dipole inversion at the PI block center. [b] Total molecular weight for two PS blocks: each PS block has M = 11.7K.

and bridge-type middle blocks, and we may be able to use this difference to estimate the bridge fraction.

On the basis of this idea, we have investigated the dielectric behavior of a polystyrene–*cis*-polyisoprene–polystyrene (PS–PI–PS) triblock copolymer having symmetrically inverted type-A dipoles in the PI block. For comparison, we also studied the behavior of a PS–PI diblock copolymer, a PS–PI/2 type prepolymer for the PS–PI–PS copolymer. Specifically, we examined the effects of a large-amplitude shear oscillation on the dielectric behavior, viscoelastic behavior, and domain alignment of the PS–PI–PS and PS–PI copolymers. Considering those effects, we attempted to estimate the bridge fraction for PS–PI–PS. The results are presented here.

Experimental Section

Materials. The PS–PI–PS sample was synthesized with a previously reported coupling method.[21] First, PS–PI$^-$Li$^+$ diblock anions were polymerized with *sec*-butyllithium in benzene. The resulting high-*cis* PI block has type-A dipoles aligned in the same direction. A fraction of the PS–PI diblock copolymer was recovered as a prepolymer, and the remaining anions were coupled with a prescribed amount of *p*-xylylene dichloride (≅95% equimolar to the anions) to produce symmetrical PS–PI–PS triblock copolymer with *dipole inversion at the midpoint of the PI block*. Finally, a small amount of the unreacted prepolymer was thoroughly removed by repeated fractionation from benzene/methanol mixtures to obtain a monodisperse PS–PI–PS copolymer sample.

The PS–PI and PS–PI–PS copolymer samples were characterized with GPC (Tosoh HLC 801A) having a refractive index monitor and an UV absorption detector. The elution solvent was THF, and commercially available monodisperse PS (Tosoh TSKs) were used as elution standards. Table 1 summarizes the characteristics of the PS–PI–PS 12–$(12)_2$–12 and PS–PI 12–12 samples. Note that the molecular structure of the PS–PI 12–12 copolymer is identical to that of a half-contour of the PS–PI–PS 12–$(12)_2$–12 copolymer. These samples (with PI content = 50%) formed lamellar microdomains, as confirmed from transmission electron micrograph (TEM) observation (cf. Figure 3).

The PI block of PS–PI 12–12 has $M_{PI} \cong M_e$ (=10K; characteristic entanglement molecular weight for PI[26]) and is barely entangled. If the middle PI block of PS–PI–PS 12–$(12)_2$–12 (with $M_{PI} \cong 2M_e$) takes a loop conformation, its dielectric as well as viscoelastic behavior should be hardly affected by entanglement, as suggested from viscoelastic data of ring polymers[27,28] having a conformation similar to the loop.

Measurements. Dielectric measurements were carried out with a capacitance bridge (GR 1615A, General Radio) for bulk films of PS–PI–PS 12–$(12)_2$–12 and PS–PI 12–12. The measurements were carried out on the films before and after imposition of a large-amplitude oscillatory strain. For this purpose, we used cone-and-plate type electrodes (of gap angle = 2.6°, diameter = 1.5 cm, and vacant capacity ≅ 20 pF) that were capable of being mounted on a laboratory rheometer having a mercury contact point. The detailed structure of this rheometer is described elsewhere.[29]

For the dielectric measurements, a prescribed amount of the PS–PI–PS and/or PS–PI sample (a little more than needed for the measurements) was slowly cast (for ca. 1 week at ≅30 °C) from a homogeneous 5 wt % toluene solution on the plate electrode placed in a half-closed chamber. After this slow-

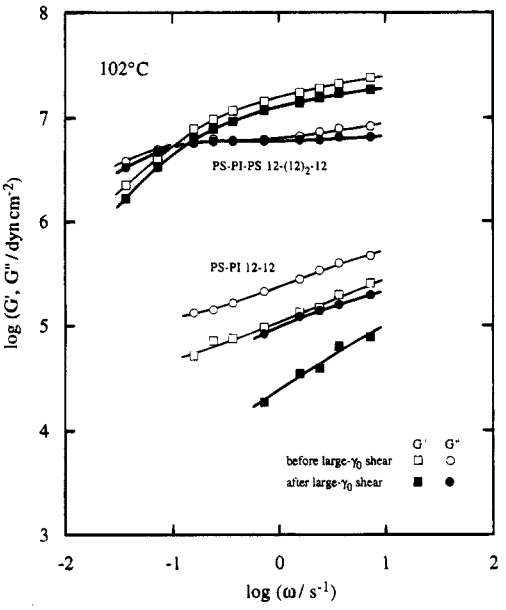

Figure 2. Dynamic viscoelastic behavior of the PS–PI–PS 12–$(12)_2$–12 and PS–PI 12–12 copolymers at 102 °C before and after the large-amplitude oscillatory shear (unfilled and filled symbols).

casting process (that helped equilibration of domain formation), the resulting as-cast film was thoroughly dried (for ca. 1 week) under vacuum at 70 °C. For TEM (JEOL 100SX), a small section was taken from the film. Then the remaining sample on the plate electrode was sandwiched with the cone electrode at 100 °C in the rheometer under a nitrogen atmosphere, rapidly cooled with a cold nitrogen stream (≅−100 °C), and subjected to a dielectric measurement at $0 \le T$ (°C) ≤ 40. After this measurement, the sample was heated to 102 °C and its dynamic viscoelastic responses were monitored against an oscillatory strain of amplitude $\gamma_0 = 0.4$. Then at the same T, the sample was subjected to ≅300 cycles of large-γ_0 oscillatory shear at $\gamma_0 = 1.15$ and $\omega = 3.67$ s^{-1}. These conditions for the large-γ_0 shear were similar to those used in previous shear-orientation studies[30] on a PS–PI copolymer similar to our PS–PI 12–12. After the large-γ_0 shear, the viscoelastic responses of the sample at 102 °C were again monitored at $\gamma_0 = 0.4$. Then the sample was rapidly cooled and again subjected to dielectric measurements at $0 \le T$ (°C) ≤ 40. Finally, TEM observation was carried out on the sheared sample.

As seen from the above experimental procedure, changes in the copolymer domain structure induced by the large-γ_0 shear were monitored by the two viscoelastic tests at $\gamma_0 = 0.4$ and TEM observations before and after the large-γ_0 shear. This enabled us to examine the shear effects on the dielectric behavior in relation to the structural and viscoelastic changes.

Results

Viscoelastic Behavior and Domain Alignment. Figure 2 shows the storage and loss moduli, G' and G'', obtained at 102 °C for the PS–PI–PS 12–$(12)_2$–12 and PS–PI 12–12 samples before and after the large-γ_0 shear. The strain amplitude for the G' and G'' data in Figure 2, $\gamma_0 = 0.4$, was not very small and the data exhibited a small nonlinearity. However, those data are useful as a monitor for the dielectric data taken just before and after G' and G'' were measured.

Figure 3 compares representative transmission electron micrographs (TEM) for the PS–PI and PS–PI–PS films before and after the large-γ_0 shear. Obviously, those TEM were taken for different sections of the films, so Figure 3 enables us to examine only qualitatively the shear effects on the domain structure.

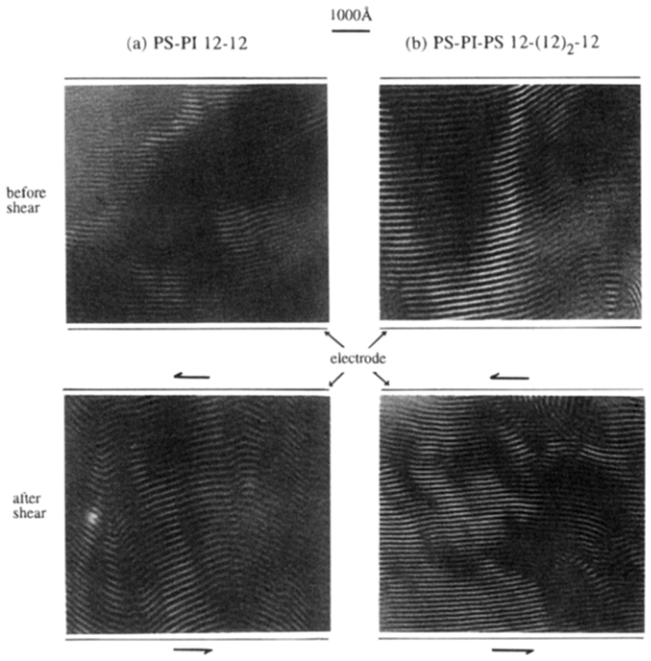

Figure 3. Representative transmission electron micrographs (TEM) for (a) PS−PI 12−12 and (b) PS−PI−PS 12−(12)$_2$−12 films before and after the large-amplitude shear oscillation. The films are stained with osmium tetraoxide.

As seen in Figure 2, the large-γ_0 shear oscillation significantly decreases G' and G'' of PS−PI 12−12 (by a factor $\delta_G \cong 3$). Essentially the same changes were found in a previous study[30] for a PS−PI 13−10 copolymer (M_{PS} = 12.5K and M_{PI} = 9.5K) being very similar to our PS−PI 12−12. That study indicated the decrease of G' and G'' to be due to shear-induced improvement of the PS−PI lamellar alignment.[30] The large-γ_0 shear conditions used here are similar to the previous conditions (shear at high ω and low T)[30c] that oriented the lamellae in a direction parallel to the shear direction. In fact, the shear appears to have improved a little the parallel alignment also for our PS−PI 12−12 (Figure 3a). Although TEM detects the domain structure only in a narrow area and scattering studies (such as SAXS) are necessary to quantify this improvement, the previous viscoelastic and structural (TEM plus SAXS) data[30] for PS−PI 13−10 enable us to qualitatively conclude the improvement for our PS−PI 12−12.

In Figures 2 and 3, we also note that the effect of the large-γ_0 shear oscillation is much smaller for PS−PI−PS 12−(12)$_2$−12 than for PS−PI 12−12: The shear decreases G' and G'' of the former only by a factor $\delta_G \cong$ 1.3 (Figure 2). Correspondingly, *under the conditions of this study*, the large-γ_0 shear appears to induce a very small change (if any) in the lamellar alignment for PS−PI−PS 12−(12)$_2$−12 (Figure 3b). As discussed later, these differences in the shear effects for the PS−PI and PS−PI−PS copolymers provide us with a clue to interpret their dielectric data.

Dielectric Behavior. Figures 4 and 5, respectively, compare dielectric loss (ϵ'') curves at 40 °C for the PS−PI−PS 12−(12)$_2$−12 (filled circles) and PS−PI 12−12 (unfilled circles) copolymers before and after imposition of the large-γ_0 oscillatory shear. The solid curve in Figure 4 indicates the ϵ'' curve of PS−PI 12−12 shifted down by a factor λ_v = 1.7, and the solid curves in Figure 5 indicate the ϵ'' data before the shear. For both PS−PI and PS−PI−PS, the time−temperature superposition was valid at $0 \le T$ (°C) ≤ 40 and the shift factor a_T was

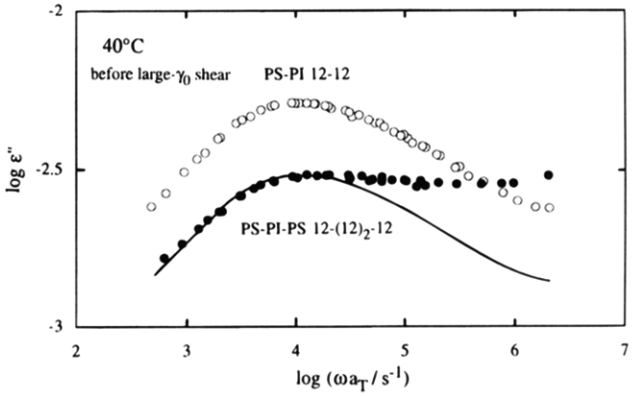

Figure 4. Dielectric loss (ϵ'') curves at 40 °C for the PS−PI 12−12 and PS−PI−PS 12−(12)$_2$−12 copolymers before the large-amplitude oscillatory shear. The solid curve indicates the ϵ'' curve of PS−PI 12−12 shifted down by a factor λ_v = 1.7.

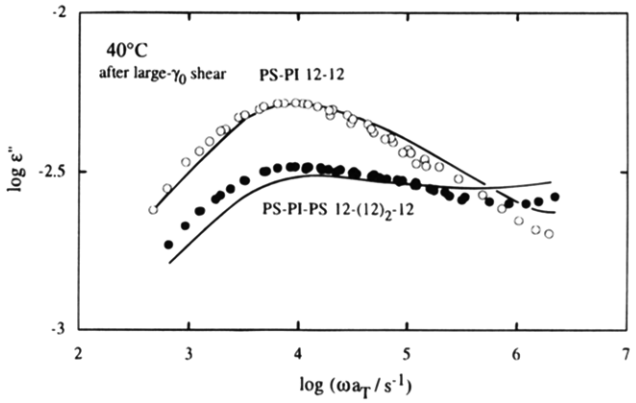

Figure 5. Dielectric loss (ϵ'') curves at 40 °C for the PS−PI 12−12 and PS−PI−PS 12−(12)$_2$−12 copolymers after the large-amplitude oscillatory shear. The solid curves indicate the data obtained before the shear (Figure 4). Although not shown here, the ϵ'' curve of PS−PI 12−12 shifted down by a factor of 1.5 was well superposed on the curve of PS−PI−PS 12−(12)$_2$−12 at low ω.

identical to that for homo-PI. This result means that the relaxation processes seen in Figures 4 and 5 are due to the *global* motion of the PI blocks connected to the glassy PS lamellae (at $T \le 40$ °C.) (The glassy PS blocks make no contribution to ϵ'', while the segmental motion of the PI blocks makes a negligible contribution at the low ω examined here.[22])

As seen in Figure 3, the PS−PI−PS and PS−PI copolymers have PI lamellae that are not perfectly but essentially parallel to the electrodes either before or after the large-γ_0 shear oscillation. Thus, the ϵ'' data seen in Figures 4 and 5 reflect the global motion of the PI blocks mostly in the direction normal to the lamella. This direction is specified as the z direction (cf. Figure 1).

For the PI block of the PS−PI 12−12 copolymer having the tail conformation, the polarization **P** is proportional to its end-to-end vector **R**. Thus, the dielectric relaxation reflects fluctuation of the z component of **R**, R_z, due to the motion of the dangling end,[22] and a normalized relaxation function is written as

$$V_{tail}(t) = \langle R_z(t)\, R_z(0)\rangle / \langle R_z^2 \rangle = \int g_{tail}(\tau) \exp(-t/\tau)\, d \ln \tau \quad \left(\int g_{tail}(\tau)\, d \ln \tau = 1\right) \quad (1)$$

Here, for convenience for later discussion, we have

introduced a relaxation mode distribution function $g_{tail}(\tau)$.

Differing from the tail PI block of PS−PI, the middle PI block of PS−PI−PS (with either the loop or the bridge conformation) has $\mathbf{P} \propto \Delta\mathbf{R} = \mathbf{R}_1 - \mathbf{R}_2$, with $\mathbf{R}_1$ and $\mathbf{R}_2$ ($=\mathbf{R} - \mathbf{R}_1$) being two end-to-center vectors (Figure 1). For this case, the dielectric relaxation detects fluctuation of ΔR_z due to the motion of the midpoint of the block (dipole inversion point), and the normalized relaxation function is given by

$$V_{middle}(t) = \langle \Delta R_z(t)\, \Delta R_z(0)\rangle / \langle \Delta R_z^2 \rangle = \int g_{middle}(\tau) \exp(-t/\tau)\, d \ln \tau \qquad (\int g_{middle}(\tau)\, d \ln \tau = 1) \quad (2)$$

The mode distribution function for the middle block, g_{middle}, is further decomposed into contributions from the loop (with fraction $1 - \phi_{bridge}$) and bridge (ϕ_{bridge}),

$$g_{middle}(\tau) = (1 - \phi_{bridge}) g_{loop}(\tau) + \phi_{bridge} g_{bridge}(\tau) \quad (3)$$

At this point, we have to emphasize that the end-to-end vector does not fluctuate for the middle PI blocks connected to the glassy PI domains. Thus, dielectric observation of the global motion of those blocks has absolutely required the dipole inversion.

For both tail and loop/bridge PI blocks, ϵ'' is related to $V(t)$ as[22]

$$\epsilon''(\omega) = -\Delta\epsilon \int_0^\infty \frac{dV(t)}{dt} \sin \omega t\, dt \quad (4)$$

where $\Delta\epsilon$ is the relaxation intensity being proportional to the magnitude of the total, active dipoles of the PI blocks involved in the unit volume. Equation 4 indicates that the ω dependence of ϵ'' (observed as the shape of the ϵ'' curve on the double-log arithmic scales in Figures 4 and 5) reflects the relaxation mode distribution of V being represented by $g(\tau)$.

We note in Figure 4 that the ϵ'' curve at *high* ω is broader for the middle PI block (filled circles) than for the tail PI block (unfilled circles), and thus the τ dependence at small τ is weaker for g_{middle} than for g_{tail}. However, we also note the coincidence of the solid curve ($\epsilon''_{PS-PI}/\lambda_v$ with $\lambda_v = 1.7$) with the filled circles at *low* ω. This result means that the middle and tail PI blocks have almost the same dielectric mode distribution at large τ but the relaxation intensity is $\cong$1.7 times smaller for the former; i.e., $g_{middle}(\tau) \cong g_{tail}(\tau)/1.7$ at large τ. As discussed later, these similarities and differences between g_{middle} and g_{tail} may be related to the loop/bridge distribution for the middle block.

In Figure 5, comparison of the data before and after the large-γ_0 shear (curves and symbols) indicates that the shear increases and decreases ϵ'' of PS−PI−PS at low and high ω, respectively, while for PS−PI the shear effect is considerably smaller, in particular at low ω. This result is in contrast to those of Figures 2 and 3: For the viscoelastic behavior and the lamellar alignment, the shear effects are much smaller for the PS−PI−PS copolymer.

After the large-γ_0 shear, the ϵ'' curve of the PS−PI 12−12 copolymer shifted down by a factor $\lambda_v = 1.5$ was well superposed on the curve of the PS−PI−PS 12−(12)$_2$−12 copolymer at low ω. Thus, after the shear $g_{middle}(\tau) \cong g_{tail}(\tau)/1.5$ at large τ, meaning that the shear reduces the difference between g_{middle} and g_{tail} (from $\lambda_v = 1.7$ to $\lambda_v = 1.5$). This reduction may be related to a shear-induced change of the loop/bridge distribution for the middle PI block, as discussed below.

Discussion

Behavior before Large-γ_0 Shear. As seen in Figure 4, the tail PI block of PS−PI 12−12 exhibits a broad dielectric relaxation: It exhibits no terminal relaxation characterized by a relationship, $\epsilon'' \propto \omega$, even at the lowest ω examined. This broad and retarded relaxation of the tail PI block is attributed to contradicting thermodynamic requirements on the PI block:[22,31] An osmotic requirement of uniform segment distribution in each microdomain forces the tail blocks to move in a highly cooperative way. During this cooperative motion, each block having a tethered end has to take a distorted conformation and violate the elastic requirement of a large conformational entropy. The resulting entropy loss works as a barrier for the motion of the tail, and the dielectric relaxation is retarded and broadened in accordance to the barrier height that is characterized with R_z for the distorted conformation (cf. Figure 1). Similar thermodynamic effects should exist also for relaxation of the middle PI block of the PS−PI−PS copolymer that takes either the loop or the bridge conformation.

At this point, we note a similarity for the loop PI block of PS−PI−PS 12−(12)$_2$−12 and the tail PI block of PS−PI 12−12: The loop is divided at its midpoint (dipole inversion point) into two fragments, each being identical to the tail. These loop fragments are anchored on the same PS domain and their end-to-end vectors always have the same z component, $R_{1z} = R_{2z}$ (Figure 1). Thus, the entropic barriers for the midpoint motion, characterized with R_{1z} and R_{2z}, should be always the same for the two loop fragments, suggesting that the two fragments together behave as a hypothetical tail for this motion and their dielectric relaxation is retarded and broadened to an extent similar to that for the tail relaxation. We also note that the two loop fragments always pull the loop midpoint in the same direction toward the PS domain on which they are anchored, and the tension and friction for the midpoint due to the respective fragment should be identical to those for the dangling end of the tail. Thus, the rate-determining factors for the block motion, the entropic barrier and the tension/friction balance, seem to be quite similar for the loop and tail examined here, and we expect their dielectric relaxation behavior to be essentially the same; i.e., $g_{loop}(\tau) \cong g_{tail}(\tau)$ (cf. eqs 1−3). (Entanglement effects are not important for the short tail and loop examined here.)

On the other hand, the above analogies with the tail do not hold for the bridge that is divided into two fragments being anchored on different PS domains. Those bridge fragments generally have $R_{1z} \neq R_{2z}$ (Figure 1) to provide different barriers for the midpoint motion, and a decrease of R_{1z} is always *canceled* by an increase of R_{2z}. Consequently, we expect that an increase of the barrier due to the motion of one bridge fragment (characterized by R_{1z}) tends to be canceled by a decrease of the barrier due to the motion of the other fragment (characterized by R_{2z}) so that the net barrier is smaller for the bridge than for the loop (which always has $R_{1z} = R_{2z}$ and does not exhibit this cancellation). Thus, the dielectric relaxation should be different for the bridge and loop: The relaxation is considered to be faster for the bridge subjected to a smaller entropic barrier, suggesting that $g_{loop}(\tau)$ overwhelms $g_{bridge}(\tau)$ at large τ.

A related difference of the bridge and loop in their mechanical responses against a stretching deformation was discussed by Halperin and Zhulina.[32]

For the PS−PI−PS 12−$(12)_2$−12 copolymer, the PI lamellar phase should include both loop and bridge. In this loop/bridge blend phase, in principle, the relaxation behavior of the loop is affected by the presence of the bridge. However, if the bridge fraction ϕ_{bridge} is rather small and this blending effect on the loop relaxation is not significant, the above argument suggests that $g_{loop}(\tau)$ for the PS−PI−PS 12−$(12)_2$−12 copolymer may be replaced by $g_{tail}(\tau)$ for PS−PI 12−12. Then we may rewrite eq 3 as

$$g_{middle}(\tau) \cong (1 - \phi_{bridge})g_{tail}(\tau) + \phi_{bridge}g_{bridge}(\tau) \cong (1 - \phi_{bridge})g_{tail}(\tau) \quad \text{at large } \tau \quad (5)$$

Equations 4 and 5 suggest that the vertical shift factor for the ϵ'' curve, $\lambda_v = 1.7$ (cf. Figure 4), provides an experimental estimate,

$$\phi_{bridge} \cong (\lambda_v - 1)/\lambda_v \cong 40\% \quad (6)$$

From eqs 4 and 5, we may also estimate $\phi_{loop} = 1 - \phi_{bridge}$ as a ratio of low-ω dielectric relaxation intensity to the total intensity of PS−PI−PS. The result was in agreement with the above estimate.

Theoretical estimates are available for ϕ_{bridge} in lamellar systems. For middle blocks taking either loop or bridge conformation, Zhulina and Halperin[14] calculated ϕ_{bridge} under a constraint for the location of the bridge midpoint. They applied an expression for the elastic energy of polymer brushes to the middle blocks and approximated the entropy of the blocks for choosing the loop/bridge conformation as an entropy of random mixing. Minimization of the resulting total free energy with respect to ϕ_{bridge} led to[14]

$$\phi_{bridge} \cong (S/a^2)^{2/3}N^{-1/3} \quad (7)$$

with S, a, and N being the surface area per block, the segment size, and half of the polymerization index for the middle block, respectively. The same result was obtained by Milner and Witten.[13] From the lamellar width (≅95 Å; Figure 3b), density (≅1 g/cm^3), and the molecular weight of the PI block, S was evaluated to be ≅200 Å^2/chain. This S value, together with $a = 6.7$ Å[33] and $N = 170$ (cf. Table 1), gives $\phi_{bridge} \cong 50\%$ (eq 7).

Equation 7 is asymptotically valid for very small S (for extremely strong segregation). For usual block copolymers, Matsen[17] has pointed out the necessity of refining the above theory by removing the constraint on the bridge midpoint and using a more accurate entropy expression for the blocks. This refinement reduces the theoretical estimate to $\phi_{bridge} \cong 40\%$.[17]

Matsen and Schick[16] used the Scheutjens−Fleer formalism for the lattice model and carried out a mean-field calculation of ϕ_{bridge}. The resulting ϕ_{bridge} depends very weakly on N and block composition (=50/50 for the copolymer examined here) and has a value ≅ 40% (cf. Figures 2−4 in ref 16).

The ϕ_{bridge} value predicted from the Matsen−Schick[16] theory and from the Zhulina−Halperin[14] and Milner−Witten[13] theories with the above refinement is in good agreement with the experimental ϕ_{bridge} value. All these theories consider the copolymer domain structures at equilibrium. The copolymers examined in this study have the order−disorder transition temperature far above 100 °C and never experienced a homogeneous state during the experiments, so one may worry about some nonequilibrium effect. However, as judged from the agreement between the experimental and theoretical domain sizes found for lamellar systems,[1,5] this effect is small for the lamellar phases. Thus, the above agreement between the experimental and theoretical ϕ_{bridge} values seems to indicate the validity of the equilibrium theories.

Effects of Large-γ_0 Shear. For the PS−PI 12−12 copolymer, the large-γ_0 shear significantly decreases G' and G'' (by the factor $\delta_G \cong 3$; Figure 2) and a little improves the lamellar alignment (Figure 3a). Nevertheless, the shear does not affect the tail population (=100%) of the end PI blocks and thus induces little change in ϵ'' (Figure 5). In contrast to those results, the PS−PI−PS 12−$(12)_2$−12 copolymer exhibits very small changes in the viscoelastic moduli (by the factor $\delta_G \cong 1.3$) and the lamellar alignment but its ϵ'' is significantly affected by the shear. This fact suggests that the shear effect on ϵ'' for PS−PI−PS 12−$(12)_2$−12 corresponds to a shear-induced change of the middle PI block conformation, i.e., a change of ϕ_{bridge}.

For PS−PI diblock lamellar systems, the large-γ_0 shear prefers smaller mechanical resistance.[30c] Thus, if the shear is applied at low T and high ω where the PS and PI lamellae have a large contrast in their viscoelastic moduli, the lamellae are aligned parallel to the shear direction so that the resulting stress is decreased.[30c] We expect a similar tendency also for the PS−PI−PS triblock lamellae: In the lamellae essentially parallel to the shear direction (cf. Figure 3b), the resistance to the shear is stronger for the bridge connecting neighboring PS domains than for the loop. Thus, the large-γ_0 shear preferring smaller resistance would decrease ϕ_{bridge}. This expectation is in harmony with the shear-induced decrease of $\lambda_v \cong 1/(1 - \phi_{bridge})$ found in Figure 5.

As done for the ϵ'' data before the large-γ_0 shear, we analyzed the data for the PS−PI−PS 12−$(12)_2$−12 copolymer in Figure 5 and estimated ϕ_{bridge} after the shear to be ≅30%. Thus, the shear decreased ϕ_{bridge} by a factor ≅1.3 (from 40 to 30%). Interestingly, this factor agrees with the reduction factor δ_G for G' and G'' of PS−PI−PS found in Figure 2. This result might be explained as follows. Similar to rubber strands, bridges exhibit an equilibrium stress that is proportional to their number density. At the frequencies of the viscoelastic test, this stress would overwhelm the stress due to the loop (and also the stress due to misalignment of lamellae as observed for PS−PI). Thus, the shear-induced decrease of ϕ_{bridge} appears to be directly reflected in the decrease of G' and G''.

Concluding Remarks

We have demonstrated that the dielectric relaxation of *dipole-inverted* PS−PI−PS can provide us with a route to evaluate the bridge fraction. This route is not limited to the triblock copolymers but is effective also for networks in general. Comparison of the dielectric data for the PI blocks of PS−PI and PS−PI−PS enabled us to estimate the bridge fraction for the latter, ϕ_{bridge} ≅ 40% (before the large-γ_0 shear), which is in good agreement with equilibrium theories. After the large-γ_0 shear, ϕ_{bridge} was decreased to ≅30%. This decrease possibly reflects the nature of shear preferring smaller mechanical resistance.

The above experimental ϕ_{bridge} values were obtained on the basis of the argument of the similarity for the loop and tail relaxation processes. Although the argu-

ment appears to be valid (at least for roughly estimating ϕ_{bridge}), the resulting ϕ_{bridge} values are dependent on the molecular picture for the loop/bridge relaxation. From this point of view, further studies are necessary to test the loop/tail similarity. Concerning this test, effects of large-amplitude shear need to be quantified for both lamellar alignment and dielectric behavior in wider ranges of shear frequency, amplitude, and temperature.

Even with the above knowledge for the shear effects, the evaluation of ϕ_{bridge} requires a molecular picture for the loop/bridge relaxation. Thus, the ϕ_{bridge} value is unavoidably affected by the choice of the picture. For this problem, we note important model systems, blends of PS−PI−PX triblock copolymer and two ring copolymers PS−PI and PX−PI, all having dipole inversion in the PI blocks. Here, PX is a block being immiscible with PS and PI. If we have the same amount of PS−PI and PX−PI rings in the blends, the three copolymers would together form PS/PI/PX trilamellar structures, and the PS−PI−PX always has bridge-PI while the PS−PI and PX−PI rings always have loop-PI. In such blends, ϕ_{bridge} is identical to the content of the PS−PI−PX copolymer. Thus, ϕ_{bridge} for the PS−PI−PS sample of our interest can be determined, without any molecular picture for loop/bridge relaxation, from the PS−PI−PX content of a particular blend that reproduces the ϵ'' data of PS−PI−PS. Studies on such model blends are considered as interesting future work.

Acknowledgment. Prof. A. Halperin at Centre de Recherches sur la Physico-Chemie des Surfaces Solides is thanked for stimulating discussion that motivated the author to use dielectric data of dipole-inverted triblock copolymers for evaluation of the bridge fraction. The author cordially thanks Mr. K. Hirose and Mr. K. Hasegawa at the Japan Synthetic Rubber Co. for generously obtaining the transmission electron micrographs and Mr. H. Yamada at Japan Advanced Institute of Science and Technology for his help with the dielectric measurements.

References and Notes

(1) Hashimoto, T. In *Polymer Alloys* 1st ed.; Kotaka, T., Ide, F., Ogino, K., Eds.; Kagaku Dojin: Tokyo, 1981; also see references therein.
(2) Hashimoto, T.; Fujimura, M.; Kawai, H. *Macromolecules* **1980**, *13*, 1660.
(3) Bates, F. S.; Fredrickson, G. H. *Annu. Rev. Phys. Chem.* **1990**, *41*, 525; also see references therein.
(4) Hashimoto, T.; Shibayama, M.; Kawai, H. *Macromolecules* **1980**, *13*, 1237.
(5) Matsushita, Y.; Mori, K.; Saguchi, R.; Nakao, Y.; Noda, I.; Nagasawa, M. *Macromolecules* **1990**, *23*, 4313.
(6) Meier, D. J. *J. Polym. Sci., Part C* **1969**, *C26*, 81.
(7) Helfand, E.; Wasserman, Z. R. *Macromolecules* **1976**, *9*, 879; **1978**, *11*, 960.
(8) Semenov, A. N. *Sov. Phys.—JETP (Engl. Transl.)* **1985**, *61*, 733.
(9) Ohta, T.; Kawasaki, K. *Macromolecules* **1986**, *19*, 2621.
(10) Spherical microdomains are smaller than the theoretical prediction. This disagreement has been attributed to nonequilibrium effects.[2]
(11) Mayes, A. M.; Olvera de la Cruz, M. *J. Chem. Phys.* **1991**, *95*, 4670.
(12) Gehlsen, M. D.; Almdal, K.; Bates, F. S. *Macromolecules* **1992**, *25*, 939.
(13) Milner, S. T.; Witten, T. A. *Macromolecules* **1992**, *25*, 5495.
(14) Zhulina, E. B.; Halperin, A. *Macromolecules* **1992**, *25*, 5730.
(15) Halperin, A. *J. Adhes.*, in press.
(16) Matsen, M. W.; Schick, M. *Macromolecules* **1994**, *27*, 187.
(17) Matsen, M. W. *J. Chem. Phys.*, in press.
(18) Stockmayer, W. H. *Pure Appl. Chem.* **1967**, *15*, 539.
(19) (a) Baur, M. E.; Stockmayer, W. H. *J. Chem. Phys.* **1965**, *43*, 4319. (b) Stockmayer, W. H.; Burke, J. J. *Macromolecules* **1969**, *2*, 647.
(20) Adachi, K.; Kotaka, T. *Prog. Polym. Sci.* **1993**, *18*, 585.
(21) Yoshida, H.; Watanabe, H.; Adachi, K.; Kotaka, T. *Macromolecules* **1991**, *24*, 2981.
(22) Yao, M.-L.; Watanabe, H.; Adachi, K.; Kotaka, T. *Macromolecules* **1991**, *24*, 2955, 6175.
(23) Watanabe, H.; Urakawa, O.; Kotaka, T. *Macromolecules* **1993**, *26*, 5073; **1994**, *27*, 3525.
(24) Boese, D.; Kremer, F.; Fetters, L. J. *Macromolecules* **1990**, *23*, 829, 1826.
(25) Patel, S. S.; Takahashi, K. M. *Macromolecules* **1992**, *25*, 4382.
(26) Graessley, W. W. *Adv. Polym. Sci.* **1974**, *16*, 1.
(27) Roovers, J. *Macromolecules* **1985**, *18*, 1359.
(28) McKenna, G. B.; Hostetter, B. J.; Hadjichristidis, N.; Fetters, L. J.; Plazek, D. J. *Macromolecules* **1989**, *22*, 1834.
(29) Watanabe, H.; Sato, T.; Osaki, K., in preparation.
(30) (a) Larson, R. G.; Winey, K. I.; Patel, S. S.; Watanabe, H.; Bruinsma, R. *Rheol. Acta* **1993**, *32*, 245. (b) Winey, K. I.; Patel, S. S.; Larson, R. G.; Watanabe, H. *Macromolecules* **1993**, *26*, 2542, 4373. (c) Patel, S. S.; Larson, R. G.; Winey, K. I.; Watanabe, H. *Macromolecules*, in press.
(31) Watanabe, H.; Kotaka, T. In *Ordering in Macromolecular Systems*; Teramoto, A., Kobayashi, M., Norisuye, T., Eds.; Springer: Berlin, 1994; p 241.
(32) Halperin, A.; Zhulina, E. B. *Europhys. Lett.* **1991**, *16*, 337.
(33) Tsunashima, Y.; Hirata, N.; Nemoto, N.; Kurata, M. *Macromolecules* **1988**, *21*, 1007.

MA9503726